Inorganic Chemistry

Article

pubs.acs.org/IC

Structures of, and Related Consequences of Deprotonation on, Two C_s-Symmetric *Arachno* Nine-Vertex Heteroboranes, 4,6-$X_2B_7H_9$ (X = CH_2; S) Studied by Gas Electron Diffraction/Quantum Chemical Calculations and GIAO/NMR

Derek A. Wann,*[,†] Paul D. Lane,[†] Heather E. Robertson,[†] Josef Holub,[‡] and Drahomír Hnyk*[,‡]

[†]School of Chemistry, University of Edinburgh, West Mains Road, Edinburgh EH9 3JJ, U.K.

[‡]Institute of Inorganic Chemistry of the Academy of Sciences of the Czech Republic, v.v.i., 250 68 Husinec-Řež, Czech Republic

Supporting Information

ABSTRACT: Gas-phase structure determinations have been performed for *arachno*-4,6-$(CH_2)_2B_7H_9$ and *arachno*-4,6-$S_2B_7H_9$ by combining quantum-chemical calculations and gas electron diffraction (GED) data. In addition, the monoanion derivatives of each of the aforementioned species have been studied using ab initio calculations. In all cases, comparison with experimental ^{11}B NMR chemical shifts have been achieved by calculating the appropriate NMR chemical shifts using GIAO-MP2 methods and the IGLO-II basis set for various geometries, both experimental and calculated. The NMR parameters calculated for the geometry obtained from the SARACEN GED refinement appeared to be quite reasonable, and in general, the fit between theoretical and experimental $\delta(^{11}B)$ NMR was found to be consistently good for all four species investigated.

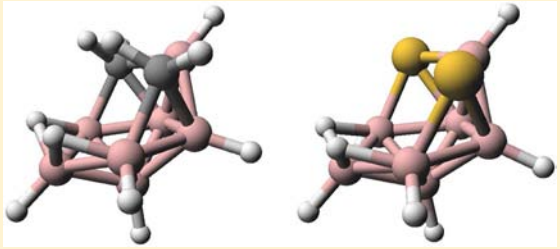

INTRODUCTION

The hypothetical nine-vertex *arachno*-$[B_9H_9]^{6-}$ would have a geometry that can be related to C_{2v}-symmetrical *closo*-$[B_{11}H_{11}]^{2-}$ through the removal of two $\{BH\}^{2+}$ vertices.[1] In this nine-vertex structure, six $\{BH\}^{2-}$ vertices occupy the open face of a hexagon, analogous to the chair conformation of cyclohexane, as shown in Figure 1. In fact, two *arachno* nine-vertex anionic borohydrides have previously been synthesized and characterized using X-ray diffraction, namely, *arachno*-$[B_9H_{13}]^{2-}$ and *arachno*-$[B_9H_{14}]^{-}$ (the former results from deprotonation of the latter).[2] Both exhibit this same geometry, but with two additional bridging hydrogen atoms and two or three extra terminal B−H bonds, respectively.

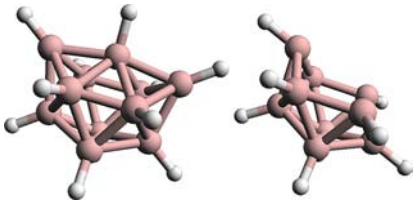

Figure 1. (left) Structure of *closo*-$[B_{11}H_{11}]^{2-}$ and (right) hypothetical structure of the nine-vertex *arachno*-$[B_9H_9]^{6-}$.

Empirical rules[3] say that $\{BH\}^{2-}$ vertices can be replaced by isoelectronic and isolobal[4] vertices such as $\{CH\}^{-}$ and $\{S\}$ at low-coordination sites. Indeed, the following substituted boranes have all been synthesized although no diffraction studies are reported: *arachno*-4,6,8-$C_2SB_8H_{10}$,[5] *arachno*-4,6-$C_2B_7H_{13}$,[6] and *arachno*-4,6-$S_2B_7H_9$.[7] That $\{CH\}^{-}$ and $\{S\}$ vertices prefer sites 4, 6, and 8 is in accordance with Gimarc's topological rule,[8] which states that elements more electronegative than boron prefer cluster sites with the highest electron density.

In general, very little is known about experimental structures of *arachno* heteroboranes. Some 10-vertex species of this cluster type, based on *arachno*-$[B_{10}H_{14}]^{2-}$, were recently studied[9,10] by employing the technique of gas electron diffraction (GED) using the SARACEN method.[11]

Recently, it was also shown that neutral *nido*-$B_{10}H_{14}$ forms a Li@$B_{10}H_{14}$ complex.[12] The borane exhibits a hexagonal open face in a boat-like conformation, rather than the chair-like conformation observed in *arachno*-4,6-$C_2B_7H_{13}$ and *arachno*-4,6-$S_2B_7H_9$. Li@$B_{10}H_{14}$ is a promising species for nonlinear optics applications.

In order to expand the family of experimentally determined *arachno* structures, we have undertaken the structural studies of *arachno*-4,6-$C_2B_7H_{13}$ and *arachno*-4,6-$S_2B_7H_9$ using the GED/SARACEN method. As these neutral species are quite prone to deprotonation, we followed computationally the reaction pathways and determined the structures of the resulting monoanions using the ab initio/GIAO/NMR method.[13] As a result of the study of $B_{10}H_{14}$ exhibiting complexation with lithium,[12] we also undertook computational investigations to

Received: December 18, 2012
Published: March 29, 2013

   dx.doi.org/10.1021/ic302776d | *Inorg. Chem.* 2013, 52, 4502−4508

see if either of the title molecules in this Article would be energetically disposed to complexation.

EXPERIMENTAL SECTION

Syntheses. Both neutral heteroboranes, 4,6-$C_2B_7H_{13}$ (**1H**) and 4,6-$S_2B_7H_9$ (**2H**), were prepared according to the literature method.[6,7] Their anions, $\mathbf{1}^-$ and $\mathbf{2}^-$, were obtained as $PSH^{(+)}$ salts from the neutral heteroboranes dissolved in hexane, by addition of the hexane solution to a proton sponge, PS [PS = 1,8-bis(dimethylamino)-naphthalene]. The precipitates were filtered off, washed with hexane, and dried in vacuo.

Computational Details. Whereas the geometries of the neutral molecules **1H** and **2H** were fully optimized in C_s point-group symmetries, optimizations of the monoanions $\mathbf{1}^-$ and $\mathbf{2}^-$ were run without symmetry constraints. The calculations for both the neutral molecules and ions were performed using the Gaussian09 suite of programs,[14] first at the RHF level with the standard 6-31G(d) basis set.[15] See Figure 2 for the structures of **1H**, $\mathbf{1}^-$, **2H**, and $\mathbf{2}^-$, showing the atom-numbering scheme. The anion $\mathbf{1}^-$ may be formed by deprotonation of **1H** in two separate ways, i.e., by removing a hydrogen atom from a B−H−B bridge or from one of the carbon atoms. Both possibilities were considered computationally. The anion $\mathbf{2}^-$ can be formed from **2H** only by removing a bridging H atom, and this was examined computationally.

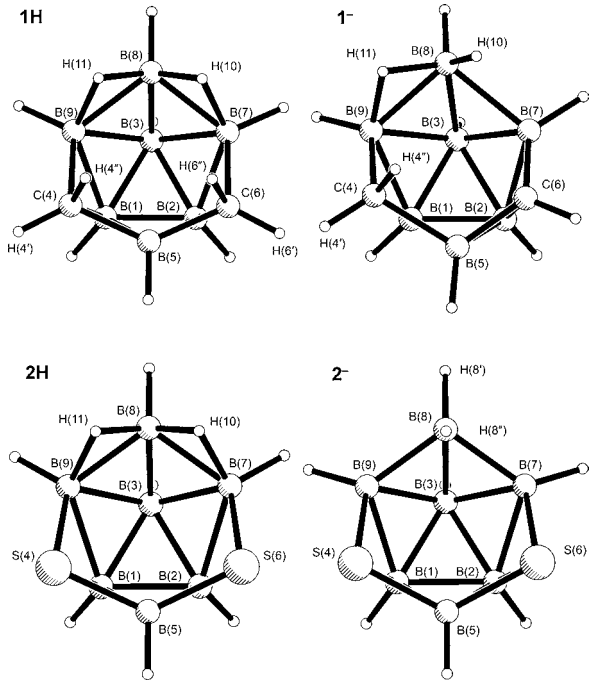

Figure 2. Molecular structures of **1H**, $\mathbf{1}^-$, **2H**, and $\mathbf{2}^-$ showing atom numbering. Hydrogen atom numbering has been omitted where the H atom has the same number as the heavy atom to which it is bonded.

The nature of any stationary points for each species was verified by frequency calculations followed by further geometry optimizations at B3LYP,[16] M06-2X,[17] and MP2(full),[18] with 6-311++G(d,p)[19] and aug-cc-pVDZ[20] basis sets. As **2H** and $\mathbf{2}^-$ contain sulfur atoms, further calculations were performed for these species at the MP2(full)/6-311++G(3df,3pd) level.

Magnetic shieldings were calculated using the GIAO-HF and GIAO-MP2[21] methods incorporated into Gaussian09 utilizing the IGLO-II basis.[22] ^{11}B chemical shifts were calculated relative to B_2H_6 and converted to the $BF_3{\cdot}OEt_2$ scale using the experimental $\delta(^{11}B)$ value for B_2H_6 of 16.6 ppm.[23]

Gas Electron Diffraction (GED). Data were collected for **1H** and **2H** using the Edinburgh GED apparatus,[24] with both species studied in a single experiment. An accelerating voltage of 40 kV was used, resulting in an electron wavelength of approximately 6 pm. Scattering intensities were recorded on Kodak Electron Image films at two nozzle-to-film distances, namely, 101.0 and 251.0 mm, to maximize the scattering angles over which data were collected. In order to obtain suitable vapor pressures and to prevent condensation in the nozzle, the sample and nozzle were heated to 100 and 115 °C, respectively, for the longer nozzle-to-film distance, and 115 and 130 °C for the shorter distance.

The weighting points for the off-diagonal weight matrices, correlation parameters, and scale factors for both camera distances are given for **1H** and **2H** in Table S1 in Supporting Information. Also included are the electron wavelengths determined using the scattering patterns for benzene, which were recorded immediately after the sample patterns. The photographic films were scanned using an Epson Expression 1680 Pro flatbed scanner as described elsewhere.[25] The data-reduction and least-squares refinement processes were carried out using the ed@ed v3.0 program[26] employing the scattering factors of Ross et al.[27]

RESULTS AND DISCUSSION

GED Structure Refinement. Molecular models were written for **1H** and **2H** converting the refinable independent parameters to Cartesian coordinates. The derivation of the model for **1H** follows essentially the same route by which it was synthesized, involving the removal of three BH vertices from *closo*-1,7-$C_2B_{10}H_{12}$,[28] and consequently relaxing the symmetry from C_{2v} to C_s. The model for **2H** was constructed in a similar manner. The calculated geometries provided further support for this modeling. The structure of **1H** was defined using 24 parameters, while **2H** required only 20 parameters as shown in Tables S2 and S3; the additional parameters required for **1H** are to define a CH_2 group rather than simply an S atom. Full descriptions of the models are given in the Supporting Information.

The GED refinements were performed using the SARACEN method,[11] incorporating flexible restraints derived from the series of calculations described earlier. Cartesian force fields were obtained from the B3LYP/6-311++G(d,p) calculations and converted to force fields described by sets of symmetry coordinates using the program SHRINK.[29] From these, the root-mean-square amplitudes of vibration (u_{h1}) and perpendicular distance corrections (k_{h1}) were generated.

For **1H**, all 24 parameters were refined; 18 of them were restrained as is normal in a SARACEN refinement to the MP2(full)/6-311++G(d,p) values, with the uncertainties in the restraints, shown in Table S2, derived from the spread of values from a series of calculations. In addition, eight groups of vibrational amplitudes were refined (see the Supporting Information, Table S3). Five of these groups were refined unrestrained, whereas each of the other three groups of amplitudes was restrained with an uncertainty of ca. 10% of its calculated [B3LYP/6-311++G(d,p)] value. The quality of fit can be assessed, numerically, from the final *R* factor (R_G) of 0.050 (R_D = 0.033) and, visually, in terms of the radial-distribution curves (Figure 3a) and the molecular scattering curves (see Figure S1).

For **2H**, all 20 parameters were refined; 15 of them were restrained to the MP2(full)/6-311++G(3df,3pd) values during refinements, as shown in Table S4. In addition, eight groups of vibrational amplitudes were refined (see Table S5). Four of these groups refined unrestrained, while each of the other four groups of amplitudes was restrained with an uncertainty of ca. 10% of its calculated value. Again, the quality of the fit can be assessed both from the final *R* factor (R_G) of 0.043 (R_D =

dx.doi.org/10.1021/ic302776d | Inorg. Chem. 2013, 52, 4502−4508

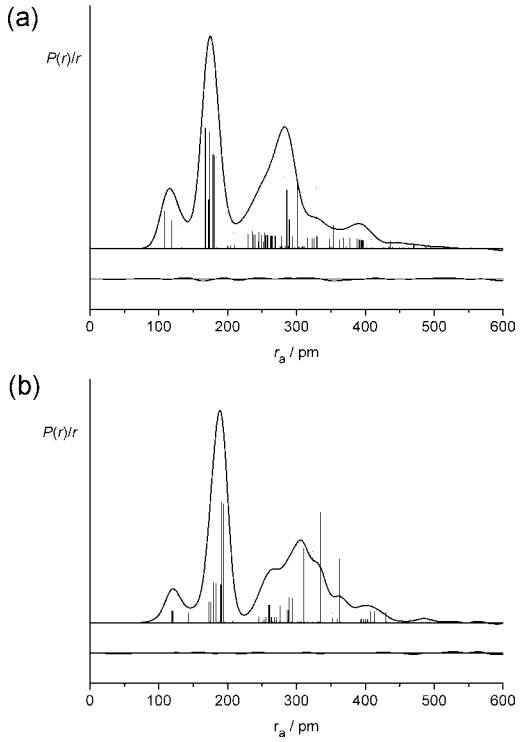

Figure 3. Experimental radial-distribution curve and theoretical-minus-experimental difference curve for the refinement of (a) **1H** and (b) **2H**. Before Fourier inversion, the data were multiplied by $s\cdot\exp(-0.00002s^2)/(Z_C - f_C)(Z_B - f_B)$ and $s\cdot\exp(-0.00002s^2)/(Z_S - f_S)(Z_B - f_B)$, respectively.

0.022) and from the radial-distribution curves (Figure 3b) and the molecular scattering curves (see Figure S2).

For both **1H** and **2H**, the refinements show good agreement between the model and experimental data. The least-squares correlation matrices are included in the Supporting Information (Tables S6 and S7).

Table 1 shows selected experimental (GED) and calculated geometric parameters for **1H**, while the equivalent data for **2H** are given in Table 2. Full sets of GED coordinates, calculated coordinates, and corresponding energies are given in Tables S8−S11.

For **1H**, the calculations were all in good agreement with the range of predicted bond lengths, typically varying by less than 2 pm. We observe that the M06-2X method consistently predicts the shortest bond lengths for the molecule, while comparison of the 6-311++G(d,p) and aug-cc-pVDZ basis sets at the MP2(full) level shows that the latter consistently predicts longer bond lengths. The angles predicted by the two basis sets are very similar. The GED results for **1H** are generally very close to the values predicted by the calculations; with all bond lengths found to be within approximately 2 pm of the values predicted by the calculations. The bond angles also show a good agreement, although the B(7)−B(2)−C(6) angle is found to differ from calculated values by ca. 4°.

For **2H**, we again find good agreement with the range of predicted bond lengths varying by less than 3 pm. We find that in comparing the three basis sets used at the MP2 level of theory that the bond lengths calculated using the 6-311++G(3df,3pd) basis set are shorter than when either the 6-311++G(d,p) or the aug-cc-pVDZ are used. Both the 6-311++G(d,p) and the aug-cc-pVDZ basis sets seem to predict longer B−S distances than using 6-311++G(3df,3pd). The GED values are again in good agreement with the calculated values, the notable exceptions being the *r*B(3)−B(8) and *r*B(2)−B(7), which vary by approximately 4 pm. As with **1H**, the bond angles show good agreement with the calculated values except for B(7)−B(2)−S(6), which again is found to differ from the calculated values by around 4°. Calculations were also performed at an MP2 level of theory with the aug-cc-pCVDZ basis set,[20,30] as we note that the MP2(full) method improves upon MP2 with frozen core mostly when core-correlation basis sets are used. Values are shown in Table 1 for comparison. However, we found that the results of these calculations provide no significant improvement on the results of the aug-cc-pVDZ, with bond lengths varying by a maximum of 0.3 pm.

Calculations were performed using the same methods for the monoanions, $\mathbf{1}^-$ and $\mathbf{2}^-$. For $\mathbf{1}^-$, there was the possibility that it had formed from **1H** either through the loss of one bridging hydrogen atom or from the loss of H from one of the CH_2 groups. Both products were optimized, and it was found that

Table 1. Selected Structural Data for 1H from the GED Refinement and Calculated Using a Variety of Theory Levels and Basis Sets[a]

	GED (r_{h1})	B3LYP/6-311++G(d,p)	M06-2X/6-311++G(d,p)	MP2(full)/aug-cc-pVDZ	MP2(full)/aug-cc-pCVDZ	MP2(full)/6-311++G(d,p)
*r*B(2)−B(3)	178.8(4)	178.6	177.9	179.6	179.3	178.4
*r*B(3)−B(7)	181.6(6)	182.4	181.0	183.0	182.7	181.7
*r*B(3)−B(8)	171.9(7)	171.1	171.1	172.5	172.2	171.4
*r*B(1)−B(2)	172.1(7)	171.2	171.4	172.8	172.5	171.7
*r*B(2)−C(6)	168.4(5)	168.0	166.6	168.1	167.9	167.3
*r*B(2)−B(7)	179.4(4)	179.5	178.4	180.2	180.0	179.1
*r*B(2)−B(5)	174.2(8)	174.1	173.8	176.1	175.8	174.7
*r*B(5)−C(6)	167.8(10)	170.5	169.5	170.2	170.1	169.8
*r*C(6)−B(7)	175.0(9)	171.7	171.4	173.2	173.1	172.3
*r*B(7)−B(8)	183.9(8)	183.5	182.0	183.3	183.1	182.4
∠B(1)−B(2)−B(7)	109.2(2)	108.9	108.6	108.6	108.6	108.6
∠B(1)−B(2)−C(6)	107.1(3)	108.3	108.0	107.7	107.7	107.8
∠B(7)−B(2)−C(6)	63.8(4)	59.1	59.4	59.5	59.6	59.5
∠Y−X−B(5)[b]	100.4(5)	100.0	100.1	100.4	100.4	100.5

[a]See Figure 2 for atom numbering. [b]X refers to the midpoint of B(1) and B(2), and Y refers to the midpoint of B(7) and B(9).

dx.doi.org/10.1021/ic302776d | *Inorg. Chem.* 2013, 52, 4502−4508

Table 2. Selected Structural Data for 2H from the GED Refinement and Calculated Using a Variety of Theory Levels and Basis Sets[a]

	GED (r_{h1})	B3LYP/6-311++G(d,p)	M06-2X/6-311++G(d,p)	MP2(full)/aug-cc-pVDZ	MP2(full)/aug-cc-pCVDZ	MP2(full)/6-311++G(d,p)	MP2(full)/6-311++G(3df,3pd)
*r*B(2)−B(3)	179.4(4)	180.1	179.2	180.8	180.6	179.6	178.5
*r*B(3)−B(7)	179.1(5)	180.2	179.1	181.0	180.8	179.7	178.8
*r*B(3)−B(8)	172.7(8)	174.1	173.8	175.5	175.3	174.3	173.0
*r*B(1)−B(2)	174.8(17)	174.2	175.0	176.3	176.0	175.1	174.5
*r*B(2)−S(6)	194.6(9)	196.2	193.8	196.1	195.9	194.2	192.5
*r*B(2)−B(7)	189.7(12)	192.3	190.0	192.3	192.2	190.5	189.7
*r*B(2)−B(5)	183.0(7)	183.2	182.2	184.5	184.2	182.5	182.1
*r*B(5)−S(6)	190.8(11)	192.0	190.4	191.4	191.2	189.9	188.5
*r*S(6)−B(7)	190.7(14)	192.7	191.2	192.5	192.5	190.5	189.6
*r*B(7)−B(8)	179.8(10)	180.9	179.8	181.2	181.0	180.3	178.6
∠B(1)−B(2)−B(7)	107.2(4)	106.9	106.6	106.6	106.7	106.6	106.5
∠B(1)−B(2)−S(6)	114.4(2)	114.3	113.9	113.7	113.7	113.7	113.8
∠B(7)−B(2)−S(6)	63.7(6)	59.4	59.8	59.4	59.5	59.5	59.5
∠Y−X−B(5)[b]	94.5(7)	94.8	95.2	94.5	94.7	94.7	94.4

[a]See Figure 2 for atom numbering. [b]X refers to the midpoint of B(1) and B(2), and Y refers to the midpoint of B(7) and B(9).

the structure formed from the removal of one hydrogen atom from the methylene group was lower in energy by 44.9 kJ mol^{-1}. For **2**$^-$, the loss of H could only have been from a bridging position.

As well as the relative energies of two possible isomers of **1**$^-$ suggesting that it is the removal of a hydrogen atom from CH_2 that leads to its formation, NMR experiments were also performed as a guide. To predict how many signals would be observed, we should first consider the removal of one bridging hydrogen atom from **1H**. Subsequent optimization of such a structure reveals rearrangement to give a geometry with C_s symmetry, thus yielding five ^{11}B NMR chemical shift signals (these were calculated to be −26.3, −24.2, −6.5, 23.7, and −49.3). However, experimental ^{11}B NMR measurements of **1**$^-$ reveal seven signals. Removal of an H atom from carbon would allow C_1 symmetry to be maintained, and that is characterized by seven $\delta(^{11}B)$ computed values, which matches the experiment (see Table 3). This isomer of **1**$^-$ is characterized

Table 3. Calculated and Experimental (in CD_3CN) ^{11}B NMR Chemical Shifts for **1**$^-$[a]

	$\delta(^{11}B)$ (ppm)						
	B(1)	B(2)	B(3)	B(5)	B(7)	B(8)	B(9)
GIAO-B3LYP/II//B3LYP/6-31G(d)	−17.9	−54.4	−40.0	−5.8	12.8	−47.7	−28.4
GIAO-HF/II//MP2/6-311G(d,p)	−13.8	−50.0	−38.4	−2.3	18.7	−40.9	−25.5
GIAO-MP2/II//MP2/6-311G(d,p)	−13.0	−49.2	−33.6	−0.5	17.5	−41.2	−24.5
experimental	−17.7	−48.5	−39.2	−3.0	8.9	−44.2	−20.0

[a]Relative to $BF_3{\cdot}OEt_2$; see text for description and Figure 2 for atom numbering.

by just one B−H−B bridge. The BH distances around what was formerly the second bridge are computed to be 121.9 and 194.9 pm, at the MP2/aug-cc-pVDZ level, demonstrating that the hydrogen atom is bonded only to one boron atom.

There is only one option for removing an H atom from **2H** to give **2**$^-$, which involves removing one of the bridging hydrogen atoms. As was the case for the high-energy isomer of **1**$^-$, **2**$^-$ has C_s symmetry, leading to five ^{11}B NMR computed and experimental resonances (see Table 4). Selected geometric

Table 4. Calculated and Experimental (in CD_3CN) ^{11}B NMR Chemical Shifts for **2**$^-$[a]

	$\delta(^{11}B)$ (ppm)				
	B(1,2)	B(3)	B(5)	B(7,9)	B(8)
GIAO-HF/II//MP2/6-31G(d)	−26.9	−11.3	2.3	15.7	−50.5
GIAO-HF/II//MP2/6-311G(d,p)	−31.8	−16.3	−2.6	10.7	−55.6
GIAO-MP2/II//MP2/6-311G(d,p)	−29.9	−15.8	1.7	14.4	−53.2
experimental	−28.8	−20.6	−1.8	11.1	−50.1

[a]Relative to $BF_3{\cdot}OEt_2$; see text for description and Figure 2 for atom numbering.

parameters for the minimum-energy isomer of **1**$^-$ and for **2**$^-$ are given in Tables 5 and 6, and calculated coordinates are given in Tables S12 and S13, Supporting Information.

The structural effects of deprotonating **1H** and **2H** to give **1**$^-$ and **2**$^-$ can be seen from comparing geometric parameters in Tables 1 and 2, with those in Tables 5 and 6. The parameters shown for **1**$^-$ and **2**$^-$ have been chosen because there are large changes upon deprotonization. Other bond lengths and angles were largely unaffected by the removal of H.

Comparison of the computational methods used for **1**$^-$ shows that, unlike for **1H**, the 6-311++G(d,p) basis set does not predict consistently shorter bond lengths than the aug-cc-pVDZ basis. Neither basis set consistently predicts shorter values, and similarly, the M06-2X method no longer always produces the shortest bond lengths of the theory levels used. The largest changes occur around C(6), the carbon atom from which the hydrogen atom has been lost, with the bond length *r*B(5)−C(6) being shortened from 169.8 pm [MP2(full)/6-311++G(d,p)] in **1H** to 155.6 pm in **1**$^-$, while *r*C(6)−B(7) has shortened from 172.3 to 154.0 pm. The distances involving the symmetrically equivalent C(4) atom in **1H** now differ significantly from those on the deprotonated carbon; *r*C(4)−B(5) has increased from 169.8 to 185.4 pm. Large structural changes are also observed around B(8), where H(10) has changed from a bridging hydrogen in **1H** to a terminal hydrogen in **1**$^-$. This results in significant lengthening of the

dx.doi.org/10.1021/ic302776d | Inorg. Chem. 2013, 52, 4502−4508

Table 5. Selected Structural Data for 1^- Calculated Using a Variety of Theory Levels and Basis Sets[a]

	B3LYP/6-311+ +G(d,p)	M06-2X/6-311+ +G(d,p)	MP2(full)/6-311+ +G(d,p)	MP2(full)/aug-cc-pVDZ
*r*B(3)−B(7)	179.9	179.9	180.3	180.8
*r*B(3)−B(9)	184.8	182.5	184.4	183.8
*r*B(3)−B(8)	179.7	178.5	181.0	179.3
*r*B(1)−B(5)	177.5	177.0	177.7	177.7
*r*B(2)−B(5)	181.5	180.8	181.7	181.7
*r*C(4)−B(5)	185.1	180.8	185.4	181.6
*r*C(6)−B(5)	154.4	154.7	155.6	155.8
*r*C(4)−B(9)	164.2	164.8	165.6	166.0
*r*C(6)−B(7)	152.9	152.9	154.0	154.5
*r*B(7)−B(8)	201.7	197.2	202.2	197.3
*r*B(8)−B(9)	190.9	188.6	190.2	187.7
∠B(1)−B(2)−B(7)	104.6	104.1	104.6	103.7
∠B(2)−B(1)−B(9)	114.7	114.2	114.5	113.9
∠B(1)−B(2)−C(6)	102.2	102.4	101.9	102.1
∠B(2)−B(1)−C(4)	116.7	115.2	116.2	115.1
∠B(7)−B(2)−C(6)	51.5	51.8	51.8	52.1
∠B(9)−B(1)−C(4)	55.3	56.1	55.8	56.3

[a]See Figure 2 for atom numbering.

bonds *r*B(3)−B(8), *r*B(8)−B(9), and *r*B(7)−B(8), with the latter increasing from 182.4 to 202.2 pm. Large changes are also seen in the bond angles with B(1)−B(2)−B(7) and B(1)−B(2)−C(6) decreasing from 108.6° and 107.8° to 104.6° and 101.9°, respectively. The formerly symmetrically equivalent angles, B(2)−B(1)−B(9) and B(2)−B(1)−C(4), have widened from 108.6° and 107.8° to 114.5° and 116.2°, respectively.

A comparison of the computational methods and basis sets for 2^- again shows that, in general, the 6-311++G(3df,3pd) basis set predicts shorter bond lengths than either 6-311++G(d,p) or aug-cc-pVDZ, with the latter reporting the longest bond lengths; the one exception is *r*B(1)−B(2), for which the 6-311++G(d,p) basis set predicts the shortest bond length. Comparing the structures of **2H** and 2^-, there are only small changes in bond lengths. The largest change is for the *r*B(3)−B(7) bond, which shortens from 178.8 to 175.4 pm [MP2(full)/6-311++G(3df,3pd)]. *r*B(1)−B(2) increases from 174.5 to 180.8 pm, while *r*S(6)−B(7) increases from 189.6 to 192.0 pm. For the *r*B(2)−B(7) bond, the smaller basis sets and lower levels of theory predict significant changes in bond lengths when comparing **2H** and 2^-, although the changes observed from the highest level calculations are much smaller. The angle B(7)−B(2)−S(6) widens from 59.5° to 61.0°, while little change is observed in the other angles.

Comparing experimental and calculated ^{11}B NMR chemical shifts will also allow us to gauge the accuracy of our GED experiments. Table 7 shows comparisons of chemical shifts based on calculated structures, the GED structures of **1H** and **2H**, and experimental values collected in CD_3CN solution. Generally, the values obtained using the GED coordinates match those from experiment reasonably well. Small differences are often observed because of the poor accuracy of the hydrogen-atom positions obtained from electron diffraction experiments. For this reason, we did further quantum chemical calculations, where the heavy atoms were fixed at GED positions, and the H atoms were optimized. Upon relaxing the hydrogen atoms attached to boron, the total energies of **1H** and **2H** were observed to lower by 25.2 and 26.4 kJ mol^{-1}, respectively. Furthermore, when the ^{11}B NMR chemical shifts were recalculated, we saw, as might be expected, that the values typically moved closer to those obtained from the computational structure. However, for **1H**, the B(7,9) and B(8) chemical-shift values are in poorer agreement with both experimental and computational values after hydrogen positions were allowed to relax.

As mentioned in the Introduction, it was recently reported that *nido*-$B_{10}H_{14}$ forms a complex with lithium.[12] We undertook a computational study to investigate the possibility of either **1H** or **2H** also forming such complexes. However, we found no significant contact to Li to occur for the chair-like hexagonal arrangements in **1H** and **2H**.

Finally, Tables 5, 6, and 7 appear to show an interesting difference when looking at the boron atom that resonates in the highest field. For both **1H** and **2H**, the ^{11}B chemical shifts are to the lowest frequencies for B(3), while for monoanionic species, it is B(2) [and to some extent for B(8)] for 1^-, and exclusively B(8) for 2^-, that exhibits the most pronounced upfield chemical shifts of ^{11}B nuclei. This is likely because of the electron distributions around the heteroatoms that lie roughly opposite the vertex being shielded. Upon deprotonization, the electron contribution to the cluster from both types of heteroatoms is changed, and another atom(s) becomes

Table 6. Selected Structural Data for 2^- Calculated Using a Variety of Theory Levels and Basis Sets[a]

	B3LYP/6-311+ +G(d,p)	M06-2X/6-311+ +G(d,p)	MP2(full)/6-311+ +G(d,p)	MP2(full)/aug-cc-pVDZ	MP2(full)/6-311+ +G(3df,3pd)
*r*B(2)−B(3)	179.3	178.8	179.2	180.4	178.3
*r*B(3)−B(7)	173.7	173.2	174.0	175.4	173.2
*r*B(3)−B(8)	175.6	174.7	175.7	176.8	174.1
*r*B(1)−B(2)	180.0	180.3	179.6	180.8	179.8
*r*B(2)−S(6)	195.3	193.0	193.4	195.4	191.8
*r*B(2)−B(7)	188.5	186.8	187.5	189.5	186.6
*r*B(2)−B(5)	185.1	184.0	184.1	184.6	183.7
*r*B(5)−S(6)	191.8	190.1	189.8	190.4	188.5
*r*S(6)−B(7)	197.2	194.8	193.5	195.5	192.0
*r*B(7)−B(8)	178.7	178.0	179.0	180.1	177.7
∠B(1)−B(2)−B(7)	106.5	106.5	106.7	106.8	106.7
∠B(1)−B(2)−S(6)	113.5	113.2	113.2	113.3	113.3
∠B(7)−B(2)−S(6)	61.8	61.7	61.0	61.0	61.0

[a]See Figure 2 for atom numbering.

dx.doi.org/10.1021/ic302776d | *Inorg. Chem.* 2013, 52, 4502−4508

Table 7. Calculated and Experimental (in CD_3CN) ^{11}B NMR Chemical Shifts for 1H/2H[a]

	$\delta(^{11}B)$ (ppm)				
	B(1,2)	B(3)	B(5)	B(7,9)	B(8)
GIAO-HF//MP2	−14.7/−22.7	−58.0/−54.7	−5.7/−6.6	−0.1/1.7	−27.0/−38.0
GIAO-MP2//MP2	−14.2/−21.7	−53.2/−48.8	0.2/−1.4	2.1/4.7	−26.5/−38.6
GIAO-HF//GED	−14.7/−23.5	−57.8/−54.0	−6.0/−4.5	1.0/2.3	−21.0/−45.2
GIAO-MP2//GED	−14.1/−22.5	−53.3/−48.0	0.3/0.6	4.0/5.2	−20.2/−46.1
GIAO-HF//GED (H relaxed)	−12.8/−23.0	−57.3/−54.7	−8.8/−5.4	2.9/1.5	−26.5/−39.1
GIAO-MP2//GED (H relaxed)	−12.2/−22.0	−52.6/−48.7	−2.8/−0.2	5.2/4.5	−25.7/−39.8
experimental	−16.3/−23.5	−51.5/−49.5	1.2/−5.0	1.8/2.4	−26.8/−38.2

[a]Relative to $BF_3{\cdot}OEt_2$; see text for description and Figure 2 for atom numbering.

opposite. This observation is pictorially demonstrated in the corresponding HOMO orbitals shown in Figure 4. Such an

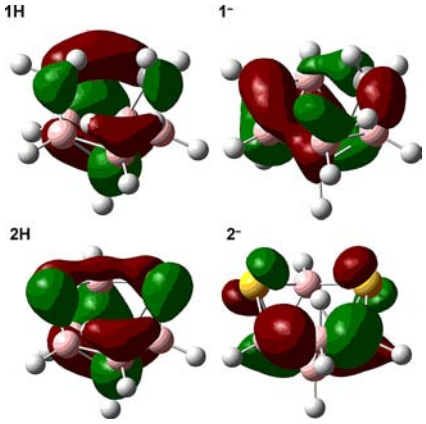

Figure 4. Highest-occupied molecular orbitals generated at the HF/6-311++G(d,p) level for **1H**, $\mathbf{1}^-$, **2H**, and $\mathbf{2}^-$.

effect was also observed, for example, for *nido*-7,8,10-$C_2SB_8H_{10}$,[31] in which the presence of an electron cloud above the open pentagonal CCBSB belt caused diamagnetic shielding of B(1), representing the very bottom of the molecule when looking down from the pentagonal ring.

■ ASSOCIATED CONTENT

Supporting Information

Additional details relating to the GED experiments (Table S1); details from the GED models and refinements, including amplitudes of vibration and curvilinear distance corrections (Tables S2−S5); least-squares correlation matrices (Tables S6−S7); final GED coordinates for **1H** and **2H** and calculated coordinates for **1H**, $\mathbf{1}^-$, **2H**, and $\mathbf{2}^-$ (Tables S8−S13); plots of molecular-scattering intensity curves (Figure S1). This material is available free of charge via the Internet at http://pubs.acs.org.

■ AUTHOR INFORMATION

Corresponding Author

*E-mail: derek.wann@ed.ac.uk (D.A.W.); hnyk@iic.cas.cz (D.H.).

Notes

The authors declare no competing financial interest.

■ ACKNOWLEDGMENTS

We thank the EPSRC for funding the electron diffraction research (EP/F037317 and EP/I004122). We would like to acknowledge the use of the EPSRC UK National Service for Computational Chemistry Software (NSCCS) at Imperial College London in carrying out this work. This work has also made use of the resources provided by the Edinburgh Compute and Data Facility (http://www.ecdf.ed.ac.uk/), which is partially supported by the eDIKT initiative (http://www.edikt.org.uk). The Royal Society of Edinburgh and the Academy of Sciences of the Czech Republic have generously supported the collaboration between D.A.W. and D.H. through their International Exchange Programme. We also appreciate the financial support of the Czech Science Foundation (project No. P208/10/2269).

■ REFERENCES

(1) The so-called "debor principle" that is derived from basic arithmetic, see Štíbr, B. *Chem. Rev.* **1992**, *92*, 225 and references therein.
(2) Getman, T. D.; Krause, J. A.; Niedenzu, P. M.; Shore, S. G. *Inorg. Chem.* **1989**, *28*, 1507 and references therein.
(3) Williams, R. E. *Adv. Inorg. Chem. Radiochem.* **1976**, *18*, 95.
(4) See, for example, Beckett, M. A.; Crook, J. E.; Kennedy, J. D. *J. Chem. Soc., Dalton Trans.* **1986**, 1879.
(5) The structure was evaluated using the ab initio/IGLO/NMR method. See, for example, Hnyk, D.; Hofmann, M.; Schleyer, P. v. R. *Collect. Czech. Chem. Commun.* **1999**, *64*, 993.
(6) Tebbe, F. N.; Garrett, P. M.; Hawthorne, M. F. *J. Am. Chem. Soc.* **1968**, *90*, 869.
(7) Plešek, J.; Heřmánek, S.; Janoušek, Z. *Collect. Czech. Chem. Commun.* **1977**, *42*, 785.
(8) Ott, J. J.; Gimarc, B. M. *J. Am. Chem. Soc.* **1986**, *108*, 4303.
(9) *arachno*-6,9-$C_2B_8H_{14}$: Hnyk, D.; Bühl, M.; Holub, J.; Gates, S. A.; Wann, D. A.; Mackie, I. D.; Borisenko, K. B.; Robertson, H. E.; Rankin, D. W. H. *Inorg. Chem.* **2006**, *45*, 6014.
(10) *arachno*-6,9-CSB_8H_{12}: Hnyk, D.; Holub, J.; Hayes, S. A.; Robinson, M. F.; Wann, D. A.; Robertson, H. E.; Rankin, D. W. H. *Inorg. Chem.* **2006**, *45*, 8442.
(11) (a) Mitzel, N. W.; Smart, B. A.; Blake, A. J.; Robertson, H. E.; Rankin, D. W. H. *J. Phys. Chem.* **1996**, *100*, 9339. (b) Blake, A. J.; Brain, P. T.; McNab, H.; Miller, J.; Morrison, C. A.; Parsons, S.; Rankin, D. W. H.; Robertson, H. E.; Smart, B. A. *J. Phys. Chem.* **1996**, *100*, 12280. (c) Mitzel, N. W.; Rankin, D. W. H. *Dalton Trans.* **2003**, 3650. (d) The first applications of SARACEN to boron cluster compounds are detailed in Brain, P. T.; Donohoe, D. J.; Hnyk, D.; Rankin, D. W. H.; Reed, D.; Reid, B. D.; Robertson, H. E.; Welch, A. J. *Inorg. Chem.* **1996**, *35*, 1701.
(12) Muhammad, S.; Xu, H.; Liao, Y.; Kan, Y.; Su, Z. *J. Am. Chem. Soc.* **2009**, *131*, 11833.
(13) See, for example, Hnyk, D.; Rankin, D. W. H. *Dalton Trans.* **2009**, 585 and references therein.
(14) Frisch, M. J.; Trucks, G. W.; Schlegel, H. B.; Scuseria, G. E.; Robb, M. A.; Cheeseman, J. R.; Scalmani, G.; Barone, V.; Mennucci, B.; Petersson, G. A.; Nakatsuji, H.; Caricato, M.; Li, X.; Hratchian, H. P.; Izmaylov, A. F.; Bloino, J.; Zheng, G.; Sonnenberg, J. L.; Hada, M.; Ehara, M.; Toyota, K.; Fukuda, R.; Hasegawa, J.; Ishida, M.; Nakajima,

dx.doi.org/10.1021/ic302776d | *Inorg. Chem.* 2013, 52, 4502−4508

T.; Honda, Y.; Kitao, O.; Nakai, H.; Vreven, T.; Montgomery, J. A., Jr.; Peralta, J. E.; Ogliaro, F.; Bearpark, M.; Heyd, J. J.; Brothers, E.; Kudin, K. N.; Staroverov, V. N.; Kobayashi, R.; Normand, J.; Raghavachari, K.; Rendell, A.; Burant, J. C.; Iyengar, S. S.; Tomasi, J.; Cossi, M.; Rega, N.; Millam, J. M.; Klene, M.; Knox, J. E.; Cross, J. B.; Bakken, V.; Adamo, C.; Jaramillo, J.; Gomperts, R.; Stratmann, R. E.; Yazyev, O.; Austin, A. J.; Cammi, R.; Pomelli, C.; Ochterski, J. W.; Martin, R. L.; Morokuma, K.; Zakrzewski, V. G.; Voth, G. A.; Salvador, P.; Dannenberg, J. J.; Dapprich, S.; Daniels, A. D.; Farkas, O.; Foresman, J. B.; Ortiz, J. V.; Cioslowski, J.; Fox, D. J. *Gaussian 09*, revision A.01; Gaussian, Inc.: Wallingford, CT, 2009.

(15) (a) Hehre, W. J.; Ditchfield, R.; Pople, J. A. *J. Chem. Phys.* **1972**, *56*, 213. (b) Hariharan, P. C.; Pople, J. A. *Theor. Chim. Acta* **1973**, *28*, 213. (c) Gordon, M. S. *Chem. Phys. Lett.* **1980**, *76*, 163.

(16) (a) Becke, A. D. *J. Chem. Phys.* **1993**, *98*, 5648. (b) Lee, C.; Yang, W.; Parr, R. G. *Phys. Rev. B* **1992**, *37*, 785.

(17) Zhao, Y.; Truhlar, D. G. *Theor. Chem. Acc.* **2008**, *120*, 215.

(18) Møller, C.; Plesset, M. S. *Phys. Rev.* **1934**, *46*, 618.

(19) (a) Krishnan, R.; Binkley, J. S.; Seeger, R.; Pople, J. A. *J. Chem. Phys.* **1980**, *72*, 650. (b) McLean, A. D.; Chandler, G. S. *J. Chem. Phys.* **1980**, *72*, 5639.

(20) (a) Dunning, T. H. *J. Chem. Phys.* **1989**, *90*, 1007. (b) Kendall, R. A.; Dunning, T. H.; Harrison, R. J. *J. Chem. Phys.* **1992**, *96*, 6796. (c) Woon, D. E.; Dunning, T. H. *J. Chem. Phys.* **1993**, *98*, 1358.

(21) (a) Ditchfield, R. *Mol. Phys.* **1974**, *27*, 789. (b) Wolinski, K.; Hinton, J. F.; Pulay, P. *J. Am. Chem. Soc.* **1990**, *112*, 8251. (c) Gauss, J. *J. Chem. Phys.* **1993**, *99*, 3629.

(22) Kutzelnigg, W.; Fleischer, U.; Schindler, M. *NMR Basic Principles and Progress*; Springer: Berlin, Germany, 1990; Vol. *23*, pp 165−262.

(23) Onak, T.; Tseng, J.; Diaz, M.; Tran, D.; Arias, J.; Herrera, S.; Brown, D. *Inorg. Chem.* **1993**, *32*, 487.

(24) Huntley, C. M.; Laurenson, G. S.; Rankin, D. W. H. *J. Chem. Soc., Dalton Trans.* **1980**, 954.

(25) Fleischer, H.; Wann, D. A.; Hinchley, S. L.; Borisenko, K. R.; Lewis, J. R.; Mawhorter, R. J.; Robertson, H. E.; Rankin, D. W. H. *Dalton Trans.* **2004**, 3221.

(26) Hinchley, S. L.; Robertson, H. E.; Borisenko, K. R.; Turner, A. R.; Johnston, B. F.; Rankin, D. W. H.; Ahmadian, M.; Jones, J. N.; Cowley, A. H. *Dalton Trans.* **2004**, 2469.

(27) Ross, A. W.; Fink, M.; Hilderbrandt, R. *International Tables for Crystallography*; Wilson, A. J. C.; Ed.; Kluwer Academic Publishers: Dordrecht, The Netherlands, 1992; Vol. *C*, p 245.

(28) Such a C_{2v}-symmetric model was used for solving the structure of closo-1,7-Cl_2-1,7-$C_2B_{10}H_{10}$; see Hnyk, D.; Brain, P. T.; Robertson, H. E.; Rankin, D. W. H.; Hofmann, M.; Schleyer, P. v. R.; Bühl, M. *J. Chem. Soc., Dalton Trans.* **1994**, 2885.

(29) Sipachev, V. A. *J. Mol. Struct.* **1985**, *121*, 143.

(30) Woon, D. E.; Dunning, T. H. *J. Chem. Phys.* **1995**, *103*, 4572.

(31) Hnyk, D.; Hofmann, M.; Schleyer, P. v. R.; Bühl, M.; Rankin, D. W. H. *J. Phys. Chem.* **1996**, *100*, 3435.